

# Quantitative Error Metrics and Test Patterns for Enhanced Dielectric Resonator Imaging of Microwave Materials

P. Korpas<sup>#§1</sup>, D. Mieczkowska<sup>§</sup>, M. Olszewska-Placha<sup>§2</sup>, J. Rudnicki<sup>§</sup>, M. Celuch<sup>§3</sup>

<sup>§</sup> QWED Sp. z o.o., Poland

<sup>#</sup> Warsaw University of Technology, Institute of Radioelectronics and Multimedia Technology, Poland

<sup>1</sup>p.korpas@ire.pw.edu.pl, <sup>2</sup>m.olszewska@qwed.eu <sup>3</sup>m.celuch@qwed.eu

**Abstract**—A quantitative criterion based on structural similarity is proposed for the quality evaluation of permittivity images obtained by the recently proposed 2D SPDR scanning technique. The criterion is shown consistent with visual quality assessment, while opening way to rigorous optimization of parameters of post-processing methods for spatial resolution improvement below the SPDR head diameter. Two test images are also defined, providing a physical insight into the SPDR imaging method and facilitating its developments.

**Keywords**—nondestructive testing, dielectric resonators, 2D scanning, microwave imaging, complex permittivity, resolution improvement, image reconstruction.

## I. INTRODUCTION

Dielectric properties of materials are essential for the design of microwave and mm-Wave components and systems. While various methods based on transmission line, quasi-free-space, microscopy tips, and resonant test fixtures are used to acquire these properties, the latter ones, and especially the split-post dielectric resonator (SPDR) method [1][2][3], are recognised for supreme accuracy [3], ease of use, and reproducibility, also in industrial environments [4]. SPDRs mounted in motorized stages have also been applied for 2D mapping of high resistivity semiconductors [2][5], but with spatial resolution of such measurements limited by the finite size of the SPDR head.

Efforts have been reported to increase the spatial resolution of SPDR images by taking advantage of the electromagnetic (EM) field distribution within the head, which can be obtained by full-wave EM modelling [6][7]. Such efforts are motivated by the interest in measuring samples smaller than the SPDR head [6][7], patterned samples [8], material inhomogeneities or inclusions. This is highly relevant to new applications of the SPDR method to energy materials, such as organic semiconductors used in solar cells [8] or graphene anodes for Li-ion batteries [9], where material nonuniformities arise from manufacturing processes, and influence the performances of target devices.

SPDR image postprocessing has been carried out in the space [7] or spatial frequency [6] domains and visual improvements of spatial resolution have been reported. Further applications of both methods have been hindered by the lack of quantitative criteria for the quality of reconstructed complex permittivity images. Moreover, optimization of the methods' parameters requires that standard test patterns be defined. This paper responds to both above needs and is organized as follows. Section II presents an experimental scanning setup [8] as applied to a small ceramic sample, image post-processing

algorithm, and Structural SIMilarity Index (SSIM) as a measure of image quality. Section III proposes two types of test patterns. SSIM Index is discussed for real and test samples, leading to the Conclusions on further applications of the SPDR imaging.

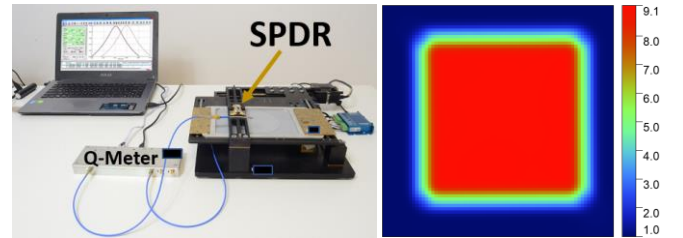


Fig. 1. 10 GHz SPDR surface scanner after [8], here applied to obtain permittivity scan of 21mm x 21 mm ceramic sample.

## II. SPDR SCANNING AND RESOLUTION ENHANCEMENT

### A. Experimental scanning

Figure 1 shows a portable laboratory setup for microwave imaging of materials with a dielectric resonator, as proposed in [8]. The SPDR is mounted into the 2D scanner and its resonant TE<sub>01δ</sub> mode at ca. 10 GHz interacts with a sample placed on the motorized table. Here, a microwave signal is generated and transmission  $|S_{21}|$  through the resonator is measured by a dedicated Microwave Frequency Q-Meter [8], but the scanner can also be used with hand-held and laboratory VNAs [10]. The measurement is controlled by a laptop application, which also extracts the resonant frequencies and Q-factors at each position of the scan, and converts them into material permittivity and loss tangent using the SPDR method [1][3], enhanced with full-wave modelling of SPDRs [7]. For SPDR head center placed at point  $(u,v)$ , the measured permittivity is denoted as  $\epsilon_{r,u,v}$  and its 2D pattern over the scanned  $n \times m$  area is written as an array (1):

$$G_{\epsilon_r} = \begin{pmatrix} \epsilon_{r,1,1} & \cdots & \epsilon_{r,1,m} \\ \vdots & \ddots & \vdots \\ \epsilon_{r,n,1} & \cdots & \epsilon_{r,n,m} \end{pmatrix}. \quad (1)$$

An analogous representation applies to the loss tangent. The image obtained for a sample of microwave ceramics is shown on the right of Fig. 1. The sample size (21 mm x 21 mm) is comparable to the size of the SPDR head (ca. 20 mm at 10 GHz), hence, close to the center of the scan the ceramic permittivity ( $\epsilon_r=9.03$ ) is correctly measured. Blurred edges are seen where the SPDR fields interact with both the ceramic and the background.

### B. Resolution enhancement by deconvolution

Spatial resolution enhancement in spatial frequency domain [6] is adapted here, based on the Wiener filter [11]:

$$H(u, v) = \frac{T^*(u, v)}{|T(u, v)|^2 + 10^{-\frac{SNR}{10}}}, \quad (2)$$

where  $T$  is SPDR template, i.e., a Fourier-transformed pattern of squared electric field in the resonator,  $SNR$  denotes an estimated value of signal-to-noise ratio in the measured data. The raw permittivity image (1) is also Fourier-transformed and the reconstructed image is obtained as:

$$\overline{G_{\epsilon_r}} = \mathcal{F}^{-1} \left\{ \mathcal{F}\{G_{\epsilon_r}\} \cdot \mathcal{F}\{H\} \right\}. \quad (3)$$

### C. Reconstruction quality metric

The Structural SIMilarity Index was proposed in [12] for quantifying image degradation caused by data compression or transmission. Subsequently, SSIM was shown relevant to the validation of a microwave tomography system [13]. It reads:

$$l(x, y) = \frac{2\mu_x\mu_y + C_1}{\mu_x^2 + \mu_y^2 + C_1}, \quad (4)$$

$$c(x, y) = \frac{2\sigma_x\sigma_y + C_2}{\sigma_x^2 + \sigma_y^2 + C_2}, \quad (5)$$

$$s(x, y) = \frac{\sigma_{xy} + \frac{C_2}{2}}{\sigma_x\sigma_y + \frac{C_2}{2}}, \quad (6)$$

$$SSIM(x, y) = [l(x, y)]^\alpha \cdot [c(x, y)]^\beta \cdot [s(x, y)]^\gamma \quad (7)$$

where  $\mu_x, \mu_y$  are average values and  $\sigma_x, \sigma_y$  - variances of the original image  $x$  and distorted  $y$ ,  $\sigma_{xy}$  is covariance,  $C_1$  and  $C_2$  - stabilizing constants,  $\alpha, \beta, \gamma$  - weights of each term of eq. (7). Here, we assume equal weights  $\alpha=\beta=\gamma=1$  and  $C_1=C_2=0$ .

The SSIM will serve to validate the reconstructed permittivity images and to indicate the approximation for SNR in the filter (2). SSIM between the actual ceramic sample (square of  $\epsilon_r=9.03$ ) and its reconstructed image (i.e., the scan of Fig. 1 subsequently resolved by (2) with different SNRs) is plotted in Fig. 2. Lack of structural similarity (SSIM $\approx$ 0) occurs if very low SNR<20dB or high SNR>80dB is assumed in (2). The best SSIM is obtained with SNR=40..50dB, which is a realistic estimate for the measurement setup of Fig. 1.

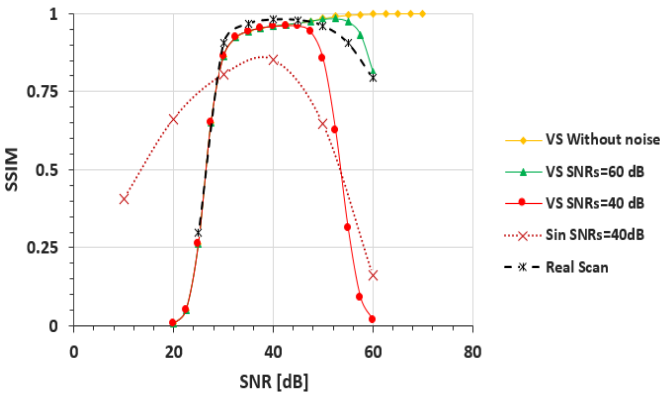


Fig. 2. Structural Similarity of different reconstructed images to their original counterparts: ceramic SUT scanned in the setup of Fig. 1 and two test patterns scanned virtually with different added noise levels.

## III. TEST PATTERNS AND VIRTUAL SCANS

### A. Preparation of Virtual Scan

Virtual scan is prepared by imitating the measurement process. Its value at position  $(u, v)$  corresponds to electric energy contained within the head of the SPDR centred at  $(u, v)$ . The details of the procedure are given in [14].

### B. Sinusoidal Test Signal and SPDR Insight

Figure 3 shows a section along a virtual sample, with areas of sinusoidal-like permittivity variation with spatial frequencies of: 0.02, 0.06, 0.1, 0.116932, 0.15, and 0.2 [periods per mm], marked on the SPDR's spatial frequency response (Fig. 3, right). A Gaussian noise of SNR=40dB is added to the virtual scan shown by the black line; the image reconstructed by filter (2) with the same SNR is shown by the green line in Fig.3.

Test frequencies are selected to demonstrate the properties of permittivity image degradation and restoration at the characteristic points. The lowest spatial frequency is captured by the SPDR with negligible attenuation. Higher frequencies are damped but filtering restores the original amplitudes (and phases) - even for the fourth pattern at the frequency of the minimum of the SPDR response, invisible in the raw scan. The SSIM of 0.85 is achieved between the original (grey) and reconstructed (green) patterns. In Fig. 2, SSIM is also plotted assuming Wiener reconstruction with different SNR in (2). For values different than the noise added to the virtual scan the SSIM is lower. This confirms that SSIM can also be used to a posteriori estimate the overall noise in the measurement system.

### C. Square Test Sample

A square sample of Fig. 4 is a digital twin of the real ceramic sample of Fig. 1. Consecutive images in Fig. 4 show its virtual scan with added 40dB noise and reconstruction with different SNR in (2). Too low SNR set in (2) leads to the damping of low frequencies; too high - amplifies the noise. For SNR in (2) equal to the actually added noise the reconstruction is the best: both visually (Fig. 4) and via SSIM (Fig. 2). Contrary to sinusoidal test patterns, maximum of SSIM is not sharp, due to different noise interaction with the different image harmonics. The optimum range is consistent for real and virtual scans, which can thus be used for optimization of SNR in (2).

## IV. CONCLUSIONS

A microwave scanning setup based on 10 GHz SPDR has been applied to the imaging of ceramic samples, with resolution enhancement achieved by deconvolution in the frequency domain. Error metrics based on structural similarity SSIM have been implemented and validated based on virtual scans of two test patterns. The first test pattern comprises sinusoids related to the SPDR transfer function and confirms the capability of the deconvolution method to restore the blurred patterns, even invisible to the eye, in the presence of a realistic 40dB noise. The second pattern is a computer model of the real ceramic, which compared to the real scan indicates the appropriate SNR for high-quality image reconstruction. The SSIM-based methodology provides a way to quantitatively compare and further develop SPDR imaging methods for novel materials.

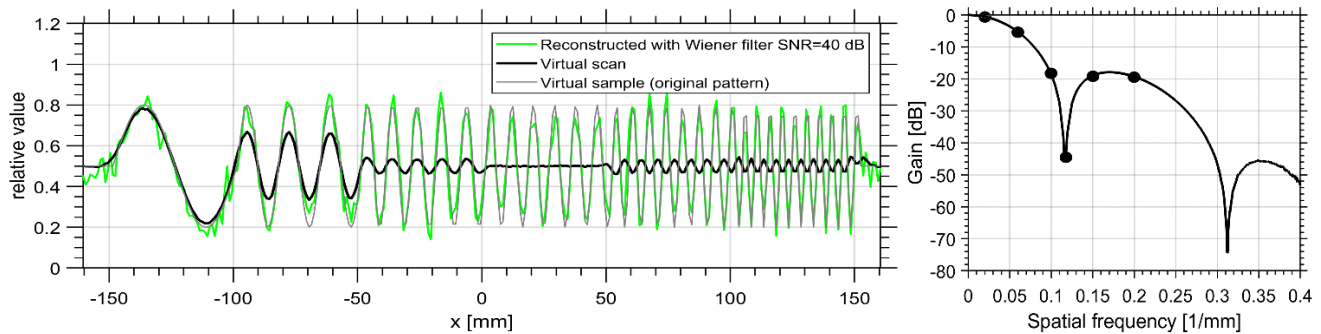


Fig. 3. Test pattern comprising sections of sinusoids (left) of different spatial frequencies marked on the 10 GHz SPDR filtering characteristic (right).

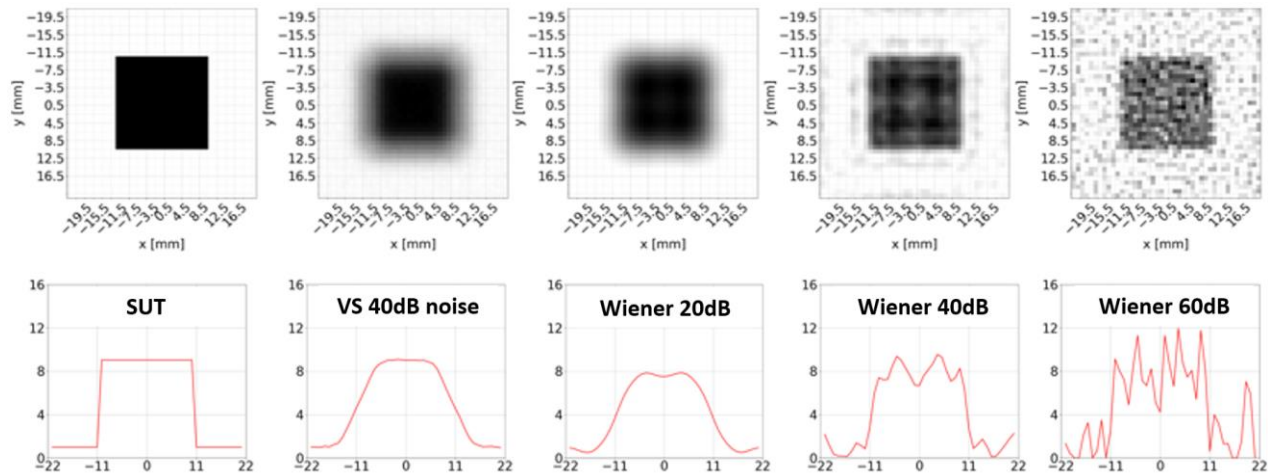


Fig. 4. From left to right: Model of the ceramic sample of Fig. 1, its virtual scan (VS) with 40dB Gaussian noise, and the results of Wiener deconvolution assuming 20dB, 40dB, and 60dB noise in eq.(2). Upper row shows 2D images and lower row shows bi-sections.

#### ACKNOWLEDGMENT

This project has received funding from the European Union's Horizon 2020 research and innovation programme under grant agreement No 861962.

#### REFERENCES

- [1] J. Krupka, A. P. Gregory, O. C. Rochard, R. N. Clarke, B. Riddle, and J. Baker-Jarvis, "Uncertainty of complex permittivity measurements by split-post dielectric resonator technique", *J. Eur. Ceramic Soc.*, vol. 21, pp. 2673-2676, 2001.
- [2] J. Krupka, D. Nguyen, and J. Mazierska, "Microwave and RF methods of contactless mapping of the sheet resistance and the complex permittivity of conductive materials and semiconductors," *Meas. Sci. Technol.*, vol. 22, no. 8, 085703, 2011.
- [3] European Standard: IEC 61189-2-721:2015. Available online: <https://webstore.iec.ch/publication/22343> (accessed on 28 Nov. 2020)
- [4] Intl. Electronics Manufacturing Initiative: "5G/mmWave Materials Assessment and Characterization Project Report 1", Nov.2020, <https://community.inemi.org/5g-electronics>
- [5] J. Krupka, W. Karcz, S. P. Avdeyev, P. Kaminski, and R. Kozlowski, "Electrical properties of deuteron irradiated high resistivity silicon", *Nucl. Instr. Methods in Physics Research B*, vol. 325, pp. 107-114, 2014. [Online]. Available: <http://dx.doi.org/10.2016/j.nimb.2014.01.21>
- [6] P. Korpas, "Deconvolution-based spatial resolution improvement technique for resistivity scans acquired with split-post dielectric resonator", *Proc. 22<sup>nd</sup> Intl. Microwave and Radar Conf. MIKON*, pp. 541-543, Poznan, PL, May 2018.
- [7] M. Celuch, W. Gwarek, and A. Wiecekowski, "Enhanced-resolution material imaging with dielectric resonators: a new implicit space-domain technique", *IEEE MTT-S International Microwave Symposium 2019*, pp. 55-58, Boston, MA, June 2019.
- [8] M. Celuch, O. Douheret, P. Korpas, R. Michnowski, M. Olszewska Placha, and J. Rudnicki, "Portable low-cost measurement setup for 2D imaging of organic semiconductors", *IEEE MTT-S International Microwave Symposium 2020*, pp. 373-376, Los Angeles, CA, Aug.2020.
- [9] H2020 NanoBat Initial Material Characterisation Report. Available online: [https://qwed.eu/nanobat\\_initial\\_material\\_characterisation.html](https://qwed.eu/nanobat_initial_material_characterisation.html) (accessed on 8 Dec.2020).
- [10] O. Stec, M. Olszewska-Placha, J. Rudnicki, and M. Celuch, "Fast and accurate extraction of complex permittivity from surface imaging with SPDR scanner and hand-held VNAs", *Proc. 23<sup>rd</sup> Intl. Microwave and Radar Conf. MIKON*, pp.181-185, Warsaw, PL, Oct. 2020.
- [11] N. Wiener, "Extrapolation, Interpolation, and Smoothing of Stationary Time Series: With Engineering Applications", The MIT Press, 1964.
- [12] Z. Wang, A. C. Bovik, H. R. Sheikh, E. P. Simoncelli, "Image quality assessment: from error visibility to structural similarity", *IEEE Transactions on Image Processing*, vol. 13, no. 4, April 2004.
- [13] A. Och, P. A. Holzl, S. Schuster, S. Scheiblhofer, D. Zankl, V. Pathuri-Bhuvana, and R. Wiegell, "High-resolution millimeter-wave Tomography system for nondestructive testing of low-permittivity materials," in *IEEE Transactions on Microwave Theory and Techniques*, doi: 10.1109/TMTT.2020.3030662
- [14] M. Celuch, W. Gwarek, and A. Wiecekowski, "Calibration software for higher-resolution dielectric resonator imaging of larger scale samples", Report D4.1. of H20202 MMAMA Project. Available online: [https://www.mmama.eu/fileadmin/user\\_upload/MMAMA\\_D4.1\\_VF.pdf](https://www.mmama.eu/fileadmin/user_upload/MMAMA_D4.1_VF.pdf) (accessed 8 Dec. 2020)